

Differences in miRNA expression profiles between GIST and leiomyoma in human samples acquired by submucosal tunneling biopsy

Authors

Koji Fujita¹, Hideki Kobara¹, Hirohito Mori¹, Shintaro Fujihara¹, Taiga Chiyo¹, Tae Matsunaga¹, Noriko Nishiyama¹, Maki Ayaki¹, Tatsuo Yachida¹, Asahiro Morishita¹, Masao Fujiwara², Keiichi Okano², Yasuyuki Suzuki², Hisakazu Iwama³, Tsutomu Masaki¹

Institutions

Institutions are listed at the end of article.

Bibliography

DOI <http://dx.doi.org/10.1055/s-0034-1393077>
Published online: 23.9.2015
Endoscopy International Open 2015; 03: E665–E671
© Georg Thieme Verlag KG
Stuttgart · New York
E-ISSN 2196-9736

Corresponding author

T. Masaki
Department of
Gastroenterology and
Neurology
Kagawa University School of
Medicine
Ikenobe 1750-1, Miki
Kagawa 761-0793
Japan
Phone: 81-87-891-2156
Fax: 81-87-891-2158
92m7v9@bma.biglobe.ne.jp

Background and study aims: Small gastrointestinal stromal tumors (GISTs) rarely have malignant potential with poor prognosis. Using conventional imaging to differentiate between small GISTs and leiomyoma, which often have similar characteristics, is difficult but essential in daily practice. Although some studies have reported on the utility of serum c-kit as a biomarker for non-small GIST and specific miRNA, clinical aspects of such testing are controversial. The aim of this study was to identify differences between small GIST and leiomyoma through the investigation of miRNA expression patterns in human cases.

Patients and methods: MiRNA expression was examined in nine GIST (less than low risk, mean 18 mm in size) samples and seven leiomyoma samples acquired by a novel sampling method, submucosal tunneling biopsy (STB), which produces tumor specimens of submucosal tumor (SMT)

without contamination of sufficient size to be examined under direct vision. Total RNA was extracted from these tissues and analyzed for miRNA expression patterns by microarray. Subsequently, real-time quantitative polymerase chain reaction (qPCR) were used to confirm specific miRNA overexpression, comparing GISTs with leiomyomas.

Results: Microarray analysis revealed upregulation of the miR-140 family up to 20 times higher in GISTs than in leiomyomas. Real-time qPCR revealed that the expression level of miR-140-5p in GISTs was 27.86 times higher than in leiomyomas; miR-140-3p was 12.24 times higher as well.

Conclusions: The STB method provided suitable SMT samples for miRNA analysis. MiR-140 family members may serve as specific biomarkers to distinguish GIST from leiomyoma.

Introduction

Early detection of tumors is crucial in cases of gastrointestinal stromal tumor (GIST) because larger tumor diameters tend to result in worse prognoses [1]. It is also important to identify GISTs at a smaller size, because even small GISTs have malignant potential with poor prognosis [2]. Each case of GIST is now subjected to surgery if possible. Thus, differentiating between GISTs and other submucosal tumors (SMTs) is essential. Leiomyomas, which are benign mesenchymal tumors located mainly in the muscular propria of the gastrointestinal tract, are difficult to differentiate from GISTs because of similar features in origin, although electron microscopy with immunohistochemistry may reveal differences [3]. Moreover, it is difficult to distinguish GISTs from leiomyomas using imaging techniques in daily practice. Serum biomarkers for GIST have not yet been established, although GISTs express specific proteins in tissues, such as c-kit and CD34 [4]. Immu-

nohistochemical analysis (i.e., c-kit staining for GIST) has furthered the accuracy of differential diagnosis of submucosal tumors [1]. Although 95% of GIST tissues express c-kit protein, the other subset presents low or negative expression [5]. Most cases of c-kit-negative GIST arise in the stomach [6]. Therefore, c-kit protein is not perfect for diagnosis of GIST, especially cases of gastric GIST. Although detection of serum c-kit by flow cytometry was reported as useful for diagnosis of GIST measuring more than 2 cm in diameter, the method has limitations in that it cannot be used to detect GIST smaller than 2 cm in diameter and cut-off levels of c-kit are not optimized in this system [7]. Genetic mutations such as *KIT* and *PDGFRA* also are associated with GIST [1]. Approximately 10% to 15% of GIST, however, do not have mutations in either *KIT* or *PDGFRA* [6]. MiRNAs have been shown to serve as biomarkers of malignant and benign diseases [8]. MiRNAs are key molecules in post-transcriptional regulation of gene expression, and alteration of miRNA ex-

License terms



pression is related to aberrant gene expression. Tumorigenesis, tumor progression, fibrosis, and tumor immunity have been described in the context of disordered miRNA expression. Accordingly, miRNA expression was previously examined in various sarcoma cases including GIST [9] and uterine leiomyoma cases [10]. A comparison of miRNA expression profiles between GISTs and leiomyosarcomas also was performed in a gastroenterology context [11]. In addition, miRNAs with altered expression levels have been identified in patients with osteosarcoma [12]. However, miRNAs specific to small GISTs classified as low risk have not been identified. Because basic approaches comparing GIST and leiomyoma may provide clinically significant findings, we aimed to identify miRNAs as biomarkers of GIST by comparing low-risk GISTs and leiomyomas of the stomach in humans.

Patients and methods

Study design

MiRNA expression was measured in nine GIST samples and seven leiomyoma samples, which were diagnosed histopathologically and acquired using a modified version of the submucosal tunneling biopsy (STB) technique [13]. STB provides the advantage of sufficient tumor specimen acquisition without contamination under direct vision. Total RNAs were extracted from these tissues and analyzed for the expression of 2,555 miRNAs by microarray, comparing GISTs with leiomyomas.

Ethics

This study was approved by the Clinical Ethics Committee of Kagawa University Hospital. All patients provided written informed consent to undergo STB and participate in the study. The use of STB was previously approved by the same ethics committee.

Clinical and pathologic information

Clinical information about the patients included gender, clinical presentation, radiologic and endoscopic findings, laboratory findings, and the pathologic characteristics of the tumors (Table 1). Immunohistochemical analysis of tissue samples was performed for c-kit, SMA, and S-100 proteins. Mitotic counts per 50 high-power fields were estimated by expert pathologists. GISTs

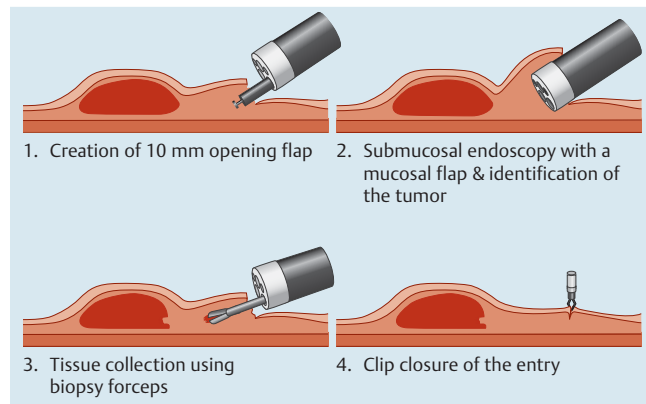


Fig. 1 Schematic protocol for submucosal tunneling biopsy. The protocol consists of four procedures: 1) creation of the entry; 2) submucosal endoscopy with a mucosal flap (SEMF), in which the tumor is identified via a submucosal tunnel; 3) core specimen (1–4 mm in size) acquisition using biopsy forceps; and 4) clip closure of the entry.

were classified according to the Fletcher [1] classification, including mitotic counts and maximum tumor size.

Submucosal tunneling biopsy

Tissue samples were obtained from patients using STB [13, 14]. This technique enables endoscopists to obtain core biopsy specimens of endoluminal subepithelial tumors under direct vision. We believe that specimens acquired with this technique are suitable for miRNA analysis because endoscopists can exclude other tissues, such as connective and adipose tissues and smooth muscle, under direct vision of the target tumors. This methodology consists of four procedures: 1) creation of the entry; 2) submucosal endoscopy with a mucosal flap (SEMF) [15]; 3) acquisition of core specimen; and 4) clip closure of the entry. These steps are shown in Fig. 1 as a schema. In short, mucosal incision using a needle knife (KD-441Q; Olympus, Tokyo, Japan), based on the endoscopic submucosal dissection (ESD) technique, was performed to create a 10-mm opening flap, followed by two-point marking of the normal mucosa around the lesion with 10-mm margins. Second, a submucosal tunnel was created by submucosal dissection toward the tumor. After the tumor was identified

Table 1 Patient profile.

Serial number	Age	Gender	Tumor location	Layer	Maximum tumor size (mm)	Echogenicity on EUS
1	76	Female	Stomach	MP	32	Hypo
2	41	Male	Stomach	MP	15	Hypo
3	72	Female	Stomach	MP	14	Hypo
4	82	Female	Stomach	MP	13	Hypo
5	73	Male	Rectum	MP	25	Hypo
6	70	Male	Stomach	MP	15	Hypo
7	48	Male	Stomach	MP	20	Hypo
8	52	Male	Stomach	MP	7.5	Hypo
9	67	Female	Stomach	MP	21	Hypo
10	54	Female	Stomach	MP	22	Hypo
11	53	Male	Stomach	MP	15	Hypo
12	66	Male	Stomach	MP	21	Hypo
13	63	Male	Stomach	MP	20	Hypo
14	69	Female	Esophagus	MP	30	Hypo
15	39	Female	Stomach	MP	10	Hypo
16	44	Male	Stomach	MP	10	Hypo

EUS: endoscopic ultrasonography; MP: muscularis propria;

and exposed under direct vision, a core specimen measuring 1 to 4 mm was acquired with biopsy forceps (Radial Jaw™ 4 Standard Capacity; Boston Scientific). Finally, the opening flap was sutured with hemoclips (HX-610–135; Olympus, Tokyo, Japan). All procedures were performed by an experienced endoscopist (H.K.; more than 200 gastric ESD cases were performed successfully).

MiRNA analysis by microarray

Total RNA was extracted from tumor tissues using the miRNeasy Mini Kit (Qiagen, Venlo, Netherland), as previously described [16]. RNA was labeled using a miRCURY Hy3 Power Labeling Kit (Exiqon, Vedbaek, Denmark) and hybridized on a human miRNA Oligo chip, version 20.0 (Toray, Tokyo). Scanning was conducted with the 3D-Gene Scanner 3000 (Toray). 3D-Gene extraction software (ver. 1.2, Toray) was used to read the raw intensity of the image. The raw data were analyzed with GeneSpringGX (ver. 10.0, Agilent Technologies, Santa Clara, CA) and quantile normalized. The microarray data obtained in this study are registered at the NCBI Gene Expression Omnibus (GEO) with the accession number GSE63453.

We calculated the fold changes in miRNA expression level between GIST and leiomyoma samples. Hierarchical clustering was accomplished using the farthest neighbor method. The uncentered Pearson's product-moment correlation coefficient was used as a metric. Statistical analysis was performed using unpaired t-tests. *P* values <0.05 were recognized as significant.

Real-time qPCR

Reverse transcription and real-time quantitative polymerase chain reaction (qPCR) were performed for miRNAs using the $\Delta\Delta$ CT method to confirm their increased expression in GISTs compared to leiomyomas, as shown in the microarray analysis. Taqman® microRNA Assays (Life technologies, Carlsbad, CA) were adapted to determine the expression level of miRNAs with U6 as an internal control (Assay ID: 001093 for U6; 001187 for miR-140–5p; 002234 for miR-140–3p). MiRNAs were reverse transcribed using the Taqman® microRNA Reverse Transcription Kit (Life Technologies) according to the manufacturer's protocol. In short, total RNA extracted using the miRNeasy Mini Kit (Qiagen) was diluted to 1.0 ng/ μ l. Reverse transcription was prepared in 15

μ l reaction consisting of 5 μ l of RNA, 3 μ l of 5 x RT primer and 12 μ l of reverse transcription master mix. As a result, 0.33 ng/ μ l of cDNA was produced. The final PCR reaction, performed in a 20- μ l-volume tube, consisted of 2 μ l of cDNA (0.66 ng), 1 μ l of 20x qPCR assay, 7 μ l of nuclease-free water and 10 μ l of Taqman® Fast Advanced Master Mix according to the manufacturer's protocol. The cDNA was amplified and quantified using StepOne Plus™ (Life technologies). MiRNA expression levels were standardized to U6.

Results



Clinical and pathologic features

The average maximum diameter of the nine GISTs was 18.05 mm, which was smaller than that of the seven leiomyomas (18.29 mm). Three of the patients with GIST presented tumors larger than 2.0 cm in diameter, and six of the nine patients presented smaller tumors. The STB method was performed successfully, providing large specimens for histopathologic assessment and total RNA extraction (Table 2). The 9 GISTs were assigned scores of 5 (very low risk) and 4 (low risk), according to the Fletcher classification (Table 3).

MiRNA analysis

To investigate candidate miRNAs as biomarkers of GIST, we screened the miRNA expression levels in GIST and leiomyoma tissues. An unsupervised hierarchical clustering analysis revealed that miRNAs in GISTs clustered separately from those in leiomyomas (Fig. 2). We identified 39 miRNAs that were differently expressed among 2,555 miRNAs examined (Table 4). In particular, 13 miRNAs were upregulated and 26 were downregulated in GISTs compared to leiomyomas. Upregulation of the miR-140 family showed the largest fold change, approximately 20-fold higher in GISTs compared to leiomyomas.

Serial number	Technical performance	Acquired specimen size (mm)	Clinical diagnosis according to Fletcher Classification
1	Success	1.4 × 1.2	GIST, low
2	Success	1.9 × 0.9	GIST, very low
3	Success	2.6 × 1.4	GIST, very low
4	Success	1.1 × 0.6	GIST, very low
5	Success	2.1 × 1.1	GIST, low
6	Success	2.2 × 2.1	GIST, very low
7	Success	1.4 × 0.9	GIST, low
8	Success	2.1 × 0.9	GIST, very low
9	Success	4.5 × 3.5	GIST, low
10	Success	2.4 × 2.0	Leiomyoma
11	Success	2.4 × 1.5	Leiomyoma
12	Success	1.9 × 1.6	Leiomyoma
13	Success		Leiomyoma
14	Success		Leiomyoma
15	Success	4.0 × 2.5	Leiomyoma
16	Success		Leiomyoma

Table 2 Sampling data obtained by submucosal tunneling biopsy.

GIST, gastrointestinal stromal tumor

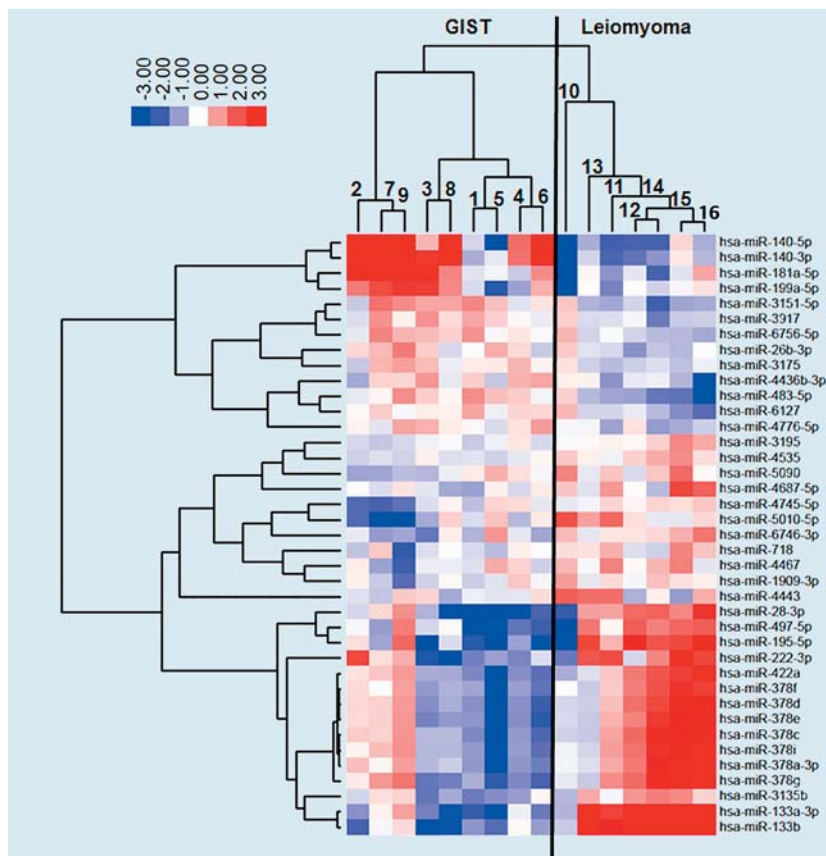


Fig. 2 Hierarchical clustering of miRNA expression profiles extracted from GIST and leiomyoma specimens acquired by submucosal tunneling biopsy. The samples are arranged in columns, and the miRNAs are arranged in rows. The tree on the left represents miRNA clustering. The tree above the heatmap shows sample clustering. The serial numbers of the samples are noted in the tree. Red squares around the serial numbers indicate the samples that were analyzed for miR-140-5p and -3p expression by real-time qPCR. Heatmaps show the relative expression intensity for each miRNA, in which the base-2 logarithm of the intensity is median-centered for each row. The color-coding is indicated as a horizontal bar at the left shoulder of the heatmap.

Table 3 Details of pathology.

Serial number	Pathologic diagnosis	Mitotic counts (/ 50 HPF)	Ki67 (M1B index)	c-kit	α -SMA	Fletcher Classification
1	GIST	<2	<3%	+	-	GIST, low
2	GIST	none <2	1%	+	-	GIST, very low
3	GIST	none <1	<2%	+	-	GIST, very low
4	GIST	none <1	1-2%	+	-	GIST, very low
5	GIST	none <1	5%	+	-	GIST, low
6	GIST	none <1	none	+	-	GIST, very low
7	GIST	none <1	<5%	+	-	GIST, low
8	GIST	<5	1-2%	+	-	GIST, very low
9	GIST	<5	<5%	+	-	GIST, low
10	Leiomyoma	none	none	-	+	Leiomyoma
11	Leiomyoma	none	none	-	+	Leiomyoma
12	Leiomyoma	none	<1%	-	+	Leiomyoma
13	Leiomyoma	none	<1%	-	+	Leiomyoma
14	Leiomyoma			-	+	Leiomyoma
15	Leiomyoma			-	+	Leiomyoma
16	Leiomyoma			-	+	Leiomyoma

GIST, gastrointestinal stromal tumor.

Real-time qPCR

Reverse transcription and real-time qPCR were performed for miR-140-5p and -3p, the two miRNAs that presented the most difference in their expression level between GIST and leiomyoma samples in the microarray analysis. The expression level of miR-140-5p compared to U6 (Δ CT \pm SD) was -1.255 ± 1.891 for GISTs and 3.545 ± 1.114 for leiomyomas ($P=0.0008$); thus, the relative expression level ($2^{-\Delta\Delta$ CT) was 27.86 times greater in GISTs compared to leiomyomas as shown in **Fig. 3**. In the case

of miR-140-3p, the Δ CT value was 5.167 ± 1.886 in GISTs and 8.780 ± 2.337 in leiomyomas ($P=0.0304$), revealing a 12.24 times greater. Samples numbered 3, 4, 6-10, 12, 14, 15, and 16 were analyzed by real-time qPCR for miR-140 family miRNAs; the other samples were not assessed because no total RNAs remained after microarray analysis.

Name	Fold change (GIST/leiomyoma)	SD	P*	Chromosomal location
miR-140-5 p	20.08	15.82	0.0099	16
miR-140-3 p	16.82	11.39	0.0040	16
miR-181a-5 p	6.18	5.10	0.0256	1
miR-199a-5 p	3.45	2.52	0.0322	19
miR-3151-5 p	2.58	1.07	0.0044	8
miR-483-5 p	2.56	0.92	0.0029	11
miR-4436b-3 p	1.77	0.66	0.0273	2
miR-6756-5 p	1.71	0.63	0.0271	11
miR-3917	1.69	0.61	0.0228	1
miR-26b-3 p	1.67	0.70	0.0488	2
miR-4776-5 p	1.65	0.54	0.0188	2
miR-3175	1.57	0.47	0.0136	15
miR-6127	1.56	0.34	0.0241	1
miR-1909-3 p	0.69	0.22	0.0378	19
miR-4745-5 p	0.66	0.32	0.0288	19
miR-3195	0.64	0.10	0.0178	20
miR-718	0.62	0.22	0.0424	X
miR-4535	0.61	0.08	0.0032	22
miR-4467	0.58	0.25	0.0372	7
miR-5090	0.56	0.22	0.0500	7
miR-6746-3 p	0.55	0.34	0.0413	11
miR-4443	0.49	0.13	0.0432	3
miR-4687-5 p	0.43	0.11	0.0412	11
miR-3135b	0.43	0.21	0.0046	6
miR-5010-5 p	0.36	0.24	0.0203	17
miR-497-5 p	0.31	0.30	0.0074	17
miR-222-3 p	0.29	0.35	0.0364	X
miR-378f	0.25	0.17	0.0072	1
miR-28-3 p	0.23	0.25	0.0050	3
miR-422a	0.23	0.18	0.0206	15
miR-378d	0.22	0.17	0.0093	4
miR-378c	0.22	0.17	0.0074	5
miR-378e	0.22	0.18	0.0090	5
miR-378g	0.22	0.21	0.0110	1
miR-378i	0.21	0.16	0.0084	22
miR-378a-3 p	0.19	0.13	0.0102	5
miR-195-5 p	0.19	0.24	0.0024	17
miR-133a-3 p	0.04	0.03	0.0016	18
miR-133b	0.03	0.02	0.0001	6

GIST, gastrointestinal stromal tumor
* Unpaired t-tests

Table 4 miRNA profiling of GIST compared to leiomyoma.

Discussion

The aim of the current study was to identify differences between small GISTs and leiomyoma through the investigation of miRNA expression patterns in human cases, because small GISTs and leiomyomas are difficult to differentially diagnose using contrast-enhanced CT scanning or endoscopic ultrasonography. Our main findings demonstrated that among 2,555 miRNAs, 13 miRNAs were upregulated and 26 miRNAs were downregulated in GISTs compared to leiomyomas. Among these, the miR-140 family was upregulated around 20 times greater in GISTs than in leiomyomas. Moreover, miRNAs extracted from tumor tissues differentially clustered between GISTs and leiomyomas. Real-time qPCR confirmed greater than a 10- to 20-fold expression of the miR-140 family in GISTs compared to leiomyomas, in accordance with the microarray analysis.

Although EUS-guided fine needle aspiration (EUS-FNA), which has emerged as a standard method for sampling submucosal tumors, has the advantages of being rapid and convenient, its diag-

nostic yield is generally limited because of too little material for immunohistochemistry and technical issues [17,18]. Accordingly, novel techniques with a greater diagnostic yield are needed to optimize tissue sampling. We have developed a novel sampling method, submucosal tunneling biopsy by using submucosal endoscopy, for gastric SMTs [13,14]. The method that is applied to create a submucosal tunnel with a safety mucosal flap [15] enables us to obtain one core specimen for immunohistologic analysis, visualization of the tumor surface [19], identification of the layer of origin, and management of hemostasis under endoscopic vision. In addition, histologic analysis demonstrated that the acquired samples were pure specimens without contamination [20] and provided suitable SMT samples for miRNA analysis in the current study. The limitation of this method is that the potential for larger and deeper fibrotic changes of mucosa following the procedure. Fibrotic adhesion between layers of mucosa may make it difficult to perform secondary endoscopic resection of the tumor [21]. Submucosal endoscopy, an endoscopic submucosal tunneling method which is recognized worldwide for use in

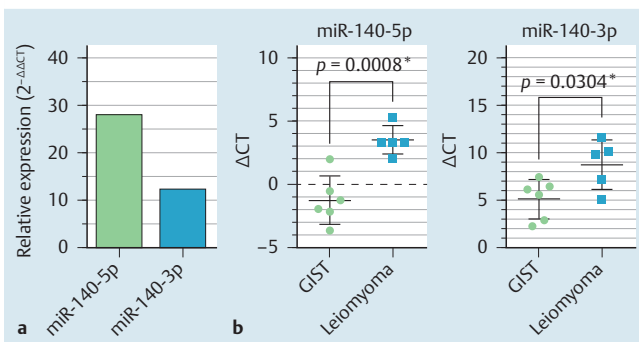


Fig. 3 Real-time qPCR for miR-140-5p and -3p in GISTs compared to leiomyomas. **a** The relative expression level ($2^{-\Delta\Delta CT}$) of miR-140-5p and -3p was higher in GISTs than leiomyomas (27.86 times and 12.24 times, respectively). **b** The expression level of the miRNAs is shown as the average $\Delta CT \pm SD$. Six GIST and five leiomyoma samples were analyzed using real-time qPCR because no total RNA remained for other GIST or leiomyoma tissues after microarray analysis. *The P values were calculated using an unpaired t-test.

oral endoscopic myotomy (POEM) [22] in patients with achalasia, has opened up the new discipline of submucosal endoscopic surgery. Through what are best termed submucosal operations, we are exploring the full potential of the outstanding diagnostic and therapeutic interventions possible in the submucosal space [21]. Thirteen miRNAs among 2,555 examined, including miR-140-5p and miR-140-3p, were upregulated in GISTs compared to leiomyomas. The miR-140 family, which presented the largest change (approximately 20 times more highly expressed in GISTs compared to leiomyomas), is expressed in mesenchymal tissues such as articular cartilage in chondrogenesis [23], human airway smooth muscle [24], and osteosarcoma [25]. MiR-140 has also been reported to regulate skeletal development. In two past studies that also reported upregulation of miR-140 family in GIST, 668 to 725 probes for miRNAs were used in microarray analysis without clear information about tumor diameter and validation of miR-140-5p/3p expression by real-time qPCR [9, 11]. Although the significance of miR-140 upregulation in GISTs remains unclear, this is the first report to identify an association between small GISTs with diameters ~20mm and miR-140 that used reliable human samples and array analysis on up to 2,555 miRNAs.

MiRNA profiling revealed miRNAs that were differentially clustered between GISTs and leiomyomas, despite the histologic similarities between these tumors. Typically, GISTs cannot be distinguished from leiomyomas without immunohistochemical examination and electron microscopy analysis [3]. Although miR-140-3p has been shown to be a poor serum biomarker in patients with osteosarcoma [12], the miR-140 family, which presented the largest change among the 39 miRNAs identified in this array analysis, should be evaluated as serum biomarkers of GIST. In addition, future studies should investigate how cartilage-specific miRNAs function in GIST and how these miRNAs contribute to the differentiation and proliferation of several mesenchymal tissues.

In conclusion, the expression profiles of the miR-140 family differed between GISTs and leiomyomas among the 2,555 miRNAs examined. MiR-140-5p and -3p may serve as specific biomarkers of small GISTs with diameters of approximately 20 mm for differential diagnosis of GISTs and leiomyomas.

Competing interests: None

Institutions

- Department of Gastroenterology and Neurology, Kagawa University School of Medicine, Kagawa, Japan
- Department of Gastroenterological Surgery, Kagawa University School of Medicine, Kagawa, Japan
- Life Science Research Center, Kagawa University School of Medicine, Kagawa, Japan

Acknowledgement

This study was supported by the UEGW2013 Top 5 abstract prize (H. Kobara).

References

- Fletcher CD, Berman JJ, Corless C et al. Diagnosis of gastrointestinal stromal tumors: A consensus approach. *Hum Pathol* 2002; 33: 459–465
- Nilsson B, Bümming P, Meis-Kindblom JM et al. Gastrointestinal stromal tumors: the incidence, prevalence, clinical course, and prognostication in the preimatinib mesylate era—a population-based study in western Sweden. *Cancer* 2005; 103: 821–829
- Franquemont DW. Differentiation and risk assessment of gastrointestinal stromal tumors. *Am J Clin Pathol* 1995; 103: 41–47
- Sircar K, Hewlett BR, Huizinga JD et al. Interstitial cells of Cajal as precursors of gastrointestinal stromal tumors. *Am J Surg Pathol* 1999; 23: 377–389
- Sarlomo-Rikala M, Kovatich AJ, Barusevicius A et al. CD117: a sensitive marker for gastrointestinal stromal tumors that is more specific than CD34. *Mod Pathol* 1998; 11: 728–734
- Yamamoto H, Oda Y. Gastrointestinal stromal tumor: recent advances in pathology and genetics. *Pathol Int* 2015; 65: 9–18
- Kakavetsi V. Seum c-kit protein detection as a reliable biomarker for the diagnosis of gastrointestinal stromal tumors. *J Mol Biomark Diagn* 2014; S6
- Weiland M, Gao XH, Zhou L et al. Small RNAs have a large impact: circulating microRNAs as biomarkers for human diseases. *RNA Biol* 2012; 9: 850–859
- Subramanian S, Lui WO, Lee CH et al. MicroRNA expression signature of human sarcomas. *Oncogene* 2008; 27: 2015–2026
- Zavadil J, Ye H, Liu Z et al. Profiling and functional analyses of microRNAs and their target gene products in human uterine leiomyomas. *PLoS One* 2010; 5: e12362
- Gits CM, van Kuijk PF, Jonkers MB et al. MiR-17-92 and miR-221/222 cluster members target KIT and ETV1 in human gastrointestinal stromal tumours. *Br J Cancer* 2013; 109: 1625–1635
- Ouyang L, Liu P, Yang S et al. A three-plasma miRNA signature serves as novel biomarkers for osteosarcoma. *Med Oncol* 2013; 30: 340
- Kobara H, Mori H, Fujiwara S et al. Bloc biopsy by tunneling method using endoscopic submucosal dissection for an upper gastrointestinal submucosal tumor. *Endoscopy* 2012; 44: E197–E198
- Kobara H, Mori H, Fujihara S et al. Bloc biopsy by using submucosal endoscopy with a mucosal flap method for gastric subepithelial tumor tissue sampling (with video). *Gastrointest Endosc* 2013; 77: 141–145
- Sumiyama K, Gostout CJ, Rajan E et al. Submucosal endoscopy with mucosal flap safety valve. *Gastrointest Endosc* 2007; 65: 688–694
- Kato K, Gong J, Iwama H et al. The antidiabetic drug metformin inhibits gastric cancer cell proliferation in vitro and in vivo. *Mol Cancer Ther* 2012; 11: 549–560
- Hoda KM, Rodriguez SA, Faigel DO. EUS-guided sampling of suspected GI stromal tumors. *Gastrointest Endosc* 2009; 69: 1218–1223
- Sepe PS, Moparty B, Pitman MB et al. EUS-guided FNA for the diagnosis of GI stromal cell tumors: sensitivity and cytologic yield. *Gastrointest Endosc* 2009; 70: 254–261
- Kobara H, Mori H, Fujihara S et al. Endoscopically visualized features of gastric submucosal tumors on submucosal endoscopy. *Endoscopy* 2014; 46: E660–E661
- Kobara H, Mori H, Rafiq K et al. Analysis of the amount of tissue sample necessary for mitotic count and Ki-67 index in gastrointestinal stromal tumor sampling. *Oncol Rep* 2015; 33: 215–222
- Khashab MA, Pasricha PJ. Conquering the third space: challenges and opportunities for diagnostic and therapeutic endoscopy. *Gastrointest Endosc* 2013; 77: 146–148

- 22 Inoue H, Minami H, Kobayashi Y et al. Peroral endoscopic myotomy (POEM) for esophageal achalasia. *Endoscopy* 2010; 42: 265–271
- 23 Karlsen TA, Jakobsen RB, Mikkelsen TS et al. microRNA-140 targets RALA and regulates chondrogenic differentiation of human mesenchymal stem cells by translational enhancement of SOX9 and ACAN. *Stem Cells Dev* 2014; 23: 290–304
- 24 Jude JA, Dileepan M, Subramanian S et al. miR-140-3p regulation of TNF- α -induced CD38 expression in human airway smooth muscle cells. *Am J Physiol Lung Cell Mol Physiol* 2012; 303: L460–L468
- 25 Song B, Wang Y, Xi Y et al. Mechanism of chemoresistance mediated by miR-140 in human osteosarcoma and colon cancer cells. *Oncogene* 2009; 28: 4065–4074